

# Solid State NMR Investigation of the Molecular Dynamics of Cocoon Silks Produced by Different *Bombyx mori* (Lepidoptera) Strains

Silvia Borsacchi,<sup>†</sup> Silvia Cappellozza,<sup>‡</sup> Donata Catalano,<sup>†</sup> Marco Geppi,<sup>\*,†</sup> and Vincenzo Ierardi<sup>†</sup>

Dipartimento di Chimica e Chimica Industriale, Università degli Studi di Pisa, v. Risorgimento 35, 56126 Pisa, Italy, and Istituto Sperimentale per la Zoologia Agraria, Sezione Specializzata per la Bachicoltura, v. dei Colli 28, 35143 Padova, Italy

Received December 30, 2005; Revised Manuscript Received February 20, 2006

Cocoons produced by different strains of *Bombyx mori* larvae were investigated by a combination of several high- and low-resolution <sup>1</sup>H and <sup>13</sup>C solid-state NMR techniques in order to characterize and compare their dynamic behavior at a molecular level. A detailed interpretation in terms of molecular motions in these very complex systems was possible thanks to the integrated analysis of different relaxation measurements and high-resolution selective experiments. Untreated cocoons of all strains were found to be mainly constituted by two different types of rigid domains and by a third one, more mobile, due to physisorbed water molecules. Dynamic processes in the MHz and kHz ranges were characterized by means of different <sup>1</sup>H and <sup>13</sup>C relaxation times. Cocoons arising from different strains exhibit a different content of physisorbed water and also slightly different dynamic behavior, especially in the MHz regime.

## Introduction

Understanding the molecular structural and dynamic properties of silk and their link with its macroscopic mechanical properties is an extraordinarily important task because of the extensive applications of this material in fields ranging from textile industry to biotechnologies. Solid-state NMR is one of the most powerful techniques for investigating both structural and dynamic properties at a molecular level, also in very complex, biomacromolecular systems. Indeed, the possibility of studying different NMR-active nuclei (for instance <sup>1</sup>H, <sup>13</sup>C, <sup>15</sup>N, and <sup>2</sup>H), as well as measuring several nuclear properties (chemical shifts, dipolar couplings, different types of relaxation times, etc.) and exploiting the huge variety of low- and high-resolution techniques nowadays available represents a solid basis for obtaining many different, very detailed microscopic information on both crystalline and amorphous domains of these systems.

Many solid state NMR studies have been performed on silks, especially by Asakura and co-workers. Most of them consist of structural studies of model peptides or isotopically enriched silks produced by different biological systems (mainly silkworms or spiders). In particular, they concern conformational analyses from <sup>13</sup>C and <sup>15</sup>N chemical shifts; determinations of torsion angles from chemical shift anisotropies, dipolar, or quadrupolar couplings or spin diffusion; and determinations of atomic distances by means of REDOR techniques.<sup>1–9</sup> On the contrary, only a few studies have been reported on the dynamic properties of silk derived from the analysis of relaxation times in nonisotopically enriched samples,<sup>10–12</sup> despite the fact that such studies were found to be particularly effective in giving insights into protein dynamics.<sup>13</sup>

The domesticated silkworm (*Bombyx mori*) silk is usually constituted of two proteins, fibroin (representing the main

component) and sericin (which coats the silk fibroin, acting as an adhesive). Notwithstanding its interesting properties, which have recently been recognized for several biotechnological applications,<sup>14,15</sup> in the past, sericin has been essentially regarded as waste, being usually removed through a degumming treatment of cocoon silk and discarded, following the procedure required by textile industrial applications. All of the solid-state NMR studies of silkworm silk have been so far performed on the sole fibroin component. Moreover, to the best of our knowledge, no comparative NMR studies have been performed on cocoons produced by different races or strains.

Here we report a <sup>1</sup>H and <sup>13</sup>C solid state NMR study of several untreated and dehydrated cocoons produced by different silkworm strains, without resorting to any isotopic labeling or cocoon physical or chemical treatment. The main aim of this work is to characterize the dynamic properties of whole cocoons (containing both fibroin and sericin) at a molecular level, with particular regard to the role played by physisorbed water, trying to detect possible differences ascribable to the different silkworm strain. To do this, we mainly resorted to the application of several low- and high-resolution techniques and, in particular, to a detailed and combined analysis of proton *T*<sub>1</sub>, *T*<sub>1ρ</sub>, and *T*<sub>2</sub> relaxation times.

## Materials and Methods

**Samples.** Three strains, belonging to the germplasm collection of the “Sezione Specializzata per la Bachicoltura di Padova”, were chosen for the experiment, by assuming the farther their geographical origin, the higher their genetical distance. The first strain, “0.208”, was imported into Italy from China in 1929 and subsequently acclimatized and selected. It is characterized by plain larvae (p/p) and golden yellow (C/C) rounded cocoons.<sup>16</sup> Hereafter throughout the text, it will be referred to as “Chinese”. The second one, “Turkish n. 28”, was imported from Turkey in 1995, and it is characterized by plain larvae (p/p) and white oval cocoons; hereafter, it will be defined as “Turkish”. The third one, imported from Japan in 1997, resembles the above-mentioned Turkish strain, since it is endowed with plain larvae (p/p) and white

\* Corresponding author. Phone: +39-050-2219289. Fax: +39-050-2219260. E-mail: mg@cci.unipi.it.

<sup>†</sup> Università degli Studi di Pisa.

<sup>‡</sup> Istituto Sperimentale per la Zoologia Agraria.

oval cocoons, but its silk production (length of silk thread) is remarkably higher. Hereafter, it will be named "Japanese".

All of the cocoon samples were prepared for the NMR analysis by separating them from mountage frames on the seventh day from spinning. Then, floss was hand-removed from the cocoons and they were hand-cut at one end, paying attention in order not to damage the pupa inside, which was subsequently gently extracted. [The "pupa" can be defined as a stage in complete metamorphosis when an insect transforms from the larval to adult stage of development; in the silkworm, the pupa is encased in a silk cocoon.] The cocoon shells were then preserved in plastic transparent bags into the dark, at 10–15 °C.

We will refer to these cocoons as "naturally hydrated" samples. Dry samples were prepared heating naturally hydrated cocoons for 2 h at 70 °C in an oven and successively storing them over P<sub>2</sub>O<sub>5</sub>.

Twenty-five cocoon shells per each strain were subjected to chemical analyses in order to determine fibroin amino acid contents; furthermore, total cocoon shells were dried, weighed, degummed in an autoclave, and weighed again after drying, to ascertain sericin-fibroin comparative percentages out of the total silk shell weight. However, no remarkable differences were found among the samples in this regard. Average fibroin composition is Gly 45.0%, Ala 28.3%, Ser 11.0%, Tyr 5.5%, other amino acids < 2.5%, with maximum variations of 0.5% for the different strains. The percentages of sericin and fibroin in the cocoons are almost the same for the three strains: 26% of sericin and 72% of fibroin for Chinese and Turkish strains and 23% of sericin and 75% of fibroin in the Japanese one; in all cases, the remaining 2% of the cocoon shell is represented by other components.

**Solid-State NMR.** <sup>13</sup>C high-resolution measurements were carried out on a two-channel Varian Infinity Plus 400 spectrometer, operating at 100.56 MHz for carbon-13 nuclei, and equipped with a 3.2 mm CP-MAS probe.

The <sup>13</sup>C spectra were recorded by spinning the sample at the magic angle with a 7 kHz frequency and under high-power <sup>1</sup>H decoupling conditions. The <sup>1</sup>H and <sup>13</sup>C 90° pulse length was 1.9 μs. In the cross-polarization (CP) experiments, a contact time of 1 ms, a relaxation delay of 2 s, and 10 000 scans were used. The direct excitation (DE) spectra were recorded using a depth pulse sequence<sup>17</sup> in order to suppress probe and rotor background signals, with 16 000 scans and a relaxation delay of 2 s, chosen to suppress the signals of carbons characterized by long <sup>13</sup>C spin–lattice relaxation times in the laboratory frame.

<sup>1</sup>H low-resolution measurements were performed on a single-channel Varian XL-100 spectrometer, operating at 25.00 MHz for proton nuclei, interfaced with a Stellar DS-NMR acquisition system and equipped with a 5 mm probe. The 90° pulse length was 2.6 μs, and in all cases, a relaxation delay of 2 s was used. The <sup>1</sup>H free induction decays (FIDs) were recorded under on-resonance conditions after application of a solid-echo pulse sequence, with an echo delay of 12 μs, a dwell time of 1 μs, and 8192 points, accumulating 4000 scans. <sup>1</sup>H spin–lattice relaxation times in the laboratory (*T*<sub>1</sub>) and rotating (*T*<sub>1ρ</sub>) frames were measured using the inversion–recovery and variable spin-lock time pulse sequences followed by solid echo, respectively. In both cases, 16 scans were accumulated, and the signal intensity was determined by the first point of the on-resonance FID. At least 27 different delays and 30 different spin-lock times were used to measure *T*<sub>1</sub> and *T*<sub>1ρ</sub>, respectively. The spin-lock field was 92 kHz. The <sup>1</sup>H *T*<sub>1ρ</sub>-FID correlation experiments were performed applying the variable spin-lock time pulse sequence followed by solid echo, using the same acquisition parameters employed to record the FID and to measure the *T*<sub>1ρ</sub>, accumulating 1000 scans, and analyzing the data as described in ref 18.

In all cases, the temperature was controlled to within 0.1 °C.

Most of the measurements were repeated for several cocoons of the same strain in order to take into account possible individual variability.

## Results and Discussion

Several high- and low-resolution NMR techniques were applied in order to investigate different structural and dynamic

properties of the cocoons at a molecular level. In particular, <sup>13</sup>C spectra mainly contain structural information, since different chemical shifts correspond to different chemical environments felt by the nuclei; however, <sup>13</sup>C spectra are also affected by dynamics, the intensity of the peaks being differently dependent, for nuclei belonging to either rigid or mobile domains, on the technique used (for instance CP-MAS or DE-MAS). <sup>1</sup>H low-resolution relaxation measurements allow dynamic behavior to be studied for molecular motions with characteristic frequencies spread over a broad range. The <sup>1</sup>H FID contains purely dynamic information, since it is not affected by the spin diffusion process. *T*<sub>2</sub>, or equivalent decay parameters, is about 10 μs in the "rigid lattice regime" (occurring when the molecular motions have characteristic frequencies lower than the static line width, usually of the order of tens of kHz), and it monotonically increases with increasing motional characteristic frequencies above this limit. Different decay FID functions correspond to dynamically distinguishable domains. On the contrary, proton spin–lattice relaxation times in the rotating (*T*<sub>1ρ</sub>) and laboratory (*T*<sub>1</sub>) frames are determined by both molecular motions and spin diffusion. Typical trends of these relaxation times with the motional frequency (or with temperature) show the occurrence of a minimum in rough correspondence with the matching between the characteristic motional frequency and either the spin-lock frequency  $\omega_1$  (for *T*<sub>1ρ</sub>, of the order of tens of kHz) or the Larmor frequency  $\omega_0$  (for *T*<sub>1</sub>, of the order of tens or hundreds MHz). Spin diffusion can partially or completely average different intrinsic proton spin–lattice relaxation times throughout the sample, giving information on the presence of heterogeneities on the 10–20 or 100–200 Å spatial scale, for *T*<sub>1ρ</sub> and *T*<sub>1</sub>, respectively.

**<sup>13</sup>C MAS Spectra.** Two kinds of <sup>13</sup>C spectra, CP- and DE-MAS, were recorded at 20 °C on both naturally hydrated and dry cocoons arising from Turkish, Japanese, and Chinese strains. They are reported in Figures 1 and 2. In the CP-MAS spectra, the signals of <sup>13</sup>C nuclei experiencing strong dipolar interactions with <sup>1</sup>H nuclei, present in the most rigid environments of the sample, are enhanced (see Figure 1). The CP-MAS spectrum of silk is characterized by a quite low resolution, mainly due to the presence of many different amino acidic residues and, for each of them, to a remarkable distribution of isotropic <sup>13</sup>C chemical shifts, arising in turn from a broad distribution of structural, conformational, and dynamic situations. Since a spectral analysis in terms of structural properties is prevented from the complexity of the spectrum, and it is indeed usually performed on isotopically labeled or model samples, we limit here the interpretation of the spectra to a summary assignment of the main groups of peaks. In particular, the following carbons, belonging to the more represented amino acidic groups, can be identified: methyl carbons of alanine (broad and asymmetric peak centered at about 21 ppm), glycine C<sub>α</sub> (≈ 43 ppm), alanine C<sub>α</sub> (≈ 50 ppm), serine and tyrosine C<sub>α</sub> (≈ 55 ppm), serine C<sub>β</sub> (≈ 62 ppm), tyrosine aromatic carbons (110–160 ppm), and carbonyl groups (≈ 171 ppm).<sup>19</sup>

It must be noticed that no remarkable differences are detected in the chemical shifts of the signals among the spectra of naturally hydrated samples of different strains. However, although the spectra of Chinese and Japanese cocoons are substantially identical, the signal at about 43 ppm, mainly ascribable to Gly amino acidic residues, is slightly less intense in the spectrum of the Turkish cocoon. To understand if this effect could be ascribed to some structural peculiarity of the Turkish cocoons or rather to a different influence of water adsorbed by the silk, we also recorded the spectra for the three

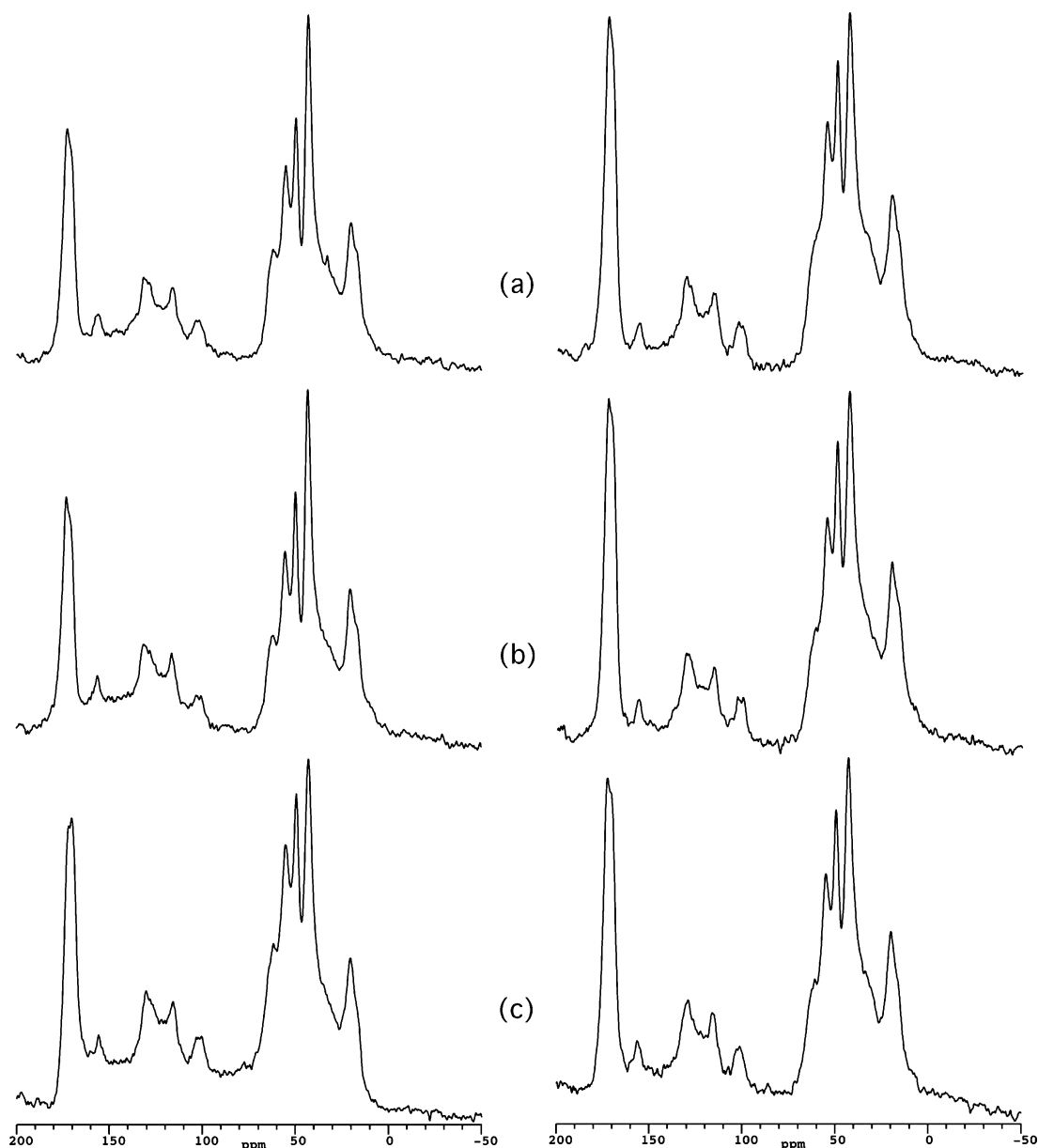


**Figure 1.**  $^{13}\text{C}$  CP-MAS spectra of (a) Chinese, (b) Japanese, and (c) Turkish cocoons, recorded for naturally hydrated (left column) and dry (right column) samples. The peaks at about 100 ppm are spinning sidebands.

dry samples. These spectra are substantially coincident, and they are also very similar to the spectrum of naturally hydrated Turkish cocoons (see Figure 1). This indicates that the presence of water affects the  $^{13}\text{C}$  spectra of Japanese and Chinese cocoons, enhancing the signal of Gly amino acidic residues, much more than that of the Turkish one:  $^1\text{H}$  FID analysis results, reported and discussed in the following, revealed that this is reasonably due to the different amount of water physisorbed by cocoons of different strains. It has been previously shown that water acts as a plasticizer of the amorphous regions of spider silk.<sup>11</sup> A change in the  $^{13}\text{C}$  CP signal intensity induced by the presence of water has already been observed for water-wetted spider silks,<sup>20,21</sup> for which the presence of a large amount of water causes a drastic reduction in the intensity of the signal ascribable to glycine, since the dramatic increase of mobility in the Gly rich, amorphous fraction of silk, strongly reduces the  $^1\text{H}$ – $^{13}\text{C}$  dipolar couplings; in our case, the slight enhancement of the glycine signal in some naturally hydrated cocoon is probably due to the opposite effect of increasing the  $^1\text{H}$ – $^{13}\text{C}$  dipolar couplings because of the presence of water protons in

the proximity of glycine  $^{13}\text{C}$  nuclei, not associated to a dramatic increase of the molecular mobility of the amorphous fibroin phase.

In the DE-MAS spectra, recorded with a very short recycle delay (2 s), the peaks arising from  $^{13}\text{C}$  nuclei with very long spin–lattice relaxation times are almost completely suppressed (see Figure 2). Such spectra almost selectively arise from the most mobile environments of the samples. The very low signal-to-noise ratio observed in these spectra with respect to the corresponding CP-MAS ones for all of the samples indicates that only a very small fraction of the cocoons is in a mobile environment. This mobile fraction is mainly represented by the methyl groups of the Ala amino acidic residues, as indicated by the predominant peak at about 21 ppm, and by other side-chain groups (the peak at about 62 ppm, mainly due to Ser  $\text{C}_\beta$ , is here more intense than those at 40–55 ppm, ascribable to main-chain carbons). However, no remarkable differences can be detected either among spectra of cocoons arising from different strains or between naturally hydrated and dry cocoons, indicating that none of these two factors (strain and presence

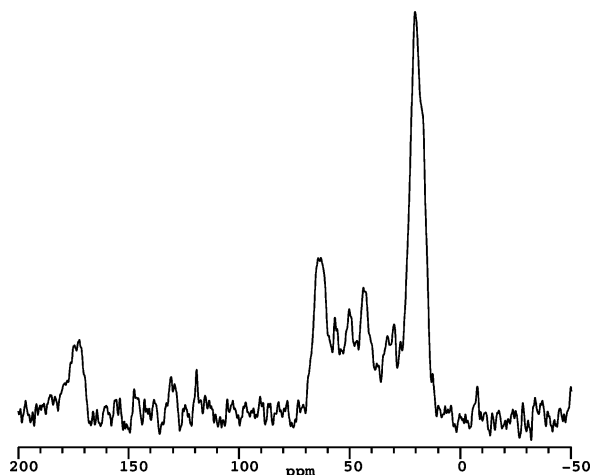


**Figure 2.**  $^{13}\text{C}$  DE-MAS spectrum of the naturally hydrated Chinese cocoon, recorded with a relaxation delay of 2 s. No appreciable differences are observed in the  $^{13}\text{C}$  DE-MAS spectra recorded in the same conditions for all of the other samples.

of water) dramatically affects the relaxation properties and the amount of the mobile side-chain groups in our samples.

**$^1\text{H}$  FID Analysis.**  $^1\text{H}$  FIDs have been recorded on resonance on both naturally hydrated and dry cocoons for all three strains at 25 °C, as well as in the temperature range 25–95 °C for all of the dry samples. To reproduce the FIDs, nonlinear least-squares fittings of the experimental decays were carried out using a linear combination of analytical functions commonly employed for this scope, chosen among exponential, Gaussian, Weibullian, Pake and, Abragamian functions.<sup>22</sup> In all cases, the best results were obtained using a sum of two exponentials and a Pake function: an example is shown in Figure 3. The analytical function used in the FID analysis can be written as

$$S(t) = w_{E1}E1(t) + w_{E2}E2(t) + w_P P(t) \quad (1)$$

where  $S(t)$  is normalized so as to be  $S(0) = 100$ ,  $w_i$  is the weight percentage of the  $i$ -type function, E1, E2, and  $P$  indicate the two exponentials and the Pake functions, respectively.

The exponential functions

$$E(t) = e^{-t/T_2} \quad (2)$$

are characterized by the spin–spin relaxation time  $T_2$ , whereas the Pake function, derived as the inverse Fourier transform of the original expression in the frequency domain,<sup>23</sup> can be written as<sup>24</sup>

$$P(t) = \sqrt{\frac{\pi}{6}} e^{-\beta^2 t^2/2} \left[ \frac{\cos \alpha t}{\sqrt{\alpha t}} C\left(\sqrt{\frac{6\alpha t}{\pi}}\right) + S\left(\sqrt{\frac{6\alpha t}{\pi}}\right) \frac{\sin \alpha t}{\sqrt{\alpha t}} \right] \quad (3)$$

where  $C$  and  $S$  are the Fresnell functions that can be approximated to<sup>25</sup>

$$C(x) \approx \frac{1}{2} + \frac{1 + 0.926x}{2 + 1.792x + 3.104x^2} \sin\left(\frac{\pi}{2}x^2\right) - \frac{1}{2 + 4.142x + 3.492x^2 + 6.670x^3} \cos\left(\frac{\pi}{2}x^2\right) \quad (4)$$

$$S(x) \approx \frac{1}{2} - \frac{1 + 0.926x}{2 + 1.792x + 3.104x^2} \cos\left(\frac{\pi}{2}x^2\right) - \frac{1}{2 + 4.142x + 3.492x^2 + 6.670x^3} \sin\left(\frac{\pi}{2}x^2\right) \quad (5)$$

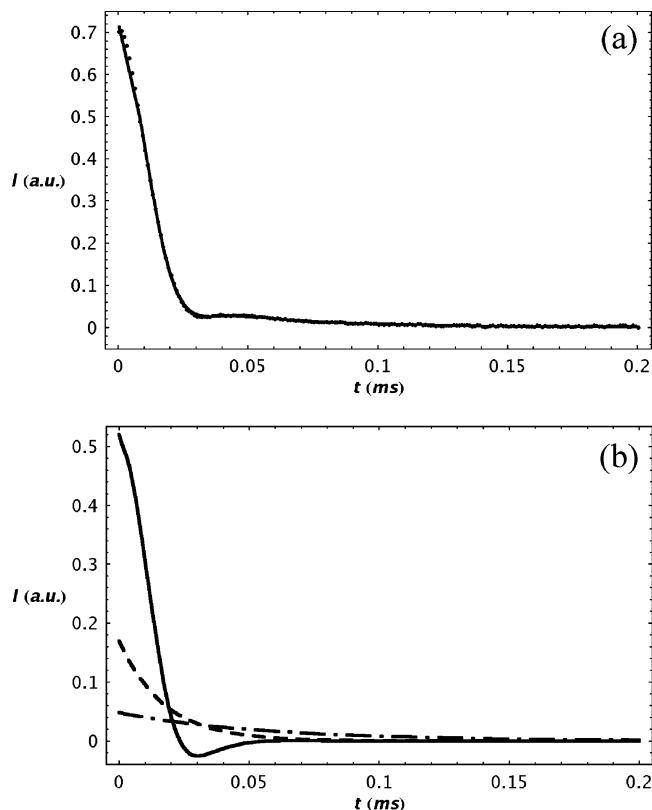


**Figure 3.** Example of  $^1\text{H}$  FID analysis. The results shown refer to the FID of the dry Japanese cocoon at 25 °C. (a) Experimental and best-fit calculated FIDs. (b) Best-fit Pake (solid line) and exponential (E1, dashed line; E2, dashed-dotted line) functions. Only the first 200 points of the FID are shown.

**Table 1.**  $^1\text{H}$  FID Analysis Results at 25 °C for Naturally Hydrated (nh) and Dry Cocoons<sup>a</sup>

samples	$w_P$ (%)	$\beta$ (s <sup>-1</sup> )	$w_{E1}$ (%)	$T_{2,E1}$ ( $\mu\text{s}$ )	$w_{E2}$ (%)	$T_{2,E2}$ ( $\mu\text{s}$ )
Chinese nh	68.4	47740	21.3	26.2	10.3	112
Japanese nh	68.3	47330	21.2	26.5	10.5	122
Turkish nh	71.9	48380	22.7	28.8	5.4	119
Chinese dry	70.5	52220	28.4	17.8	1.1	143
Japanese dry	69.8	51340	23.6	17.1	6.6	55.0
Turkish dry	75.6	52580	23.4	21.7	1.0	124

<sup>a</sup> Estimated maximum error on weight percentages is 1%, while  $\beta$  and  $T_2$  are determined with an uncertainty of about 1 and 10%, respectively.

and  $\alpha = 3\gamma^2\hbar/4R_{\text{HH}}^3$ , where  $\gamma$  is the proton gyromagnetic ratio. The Pake function is therefore characterized by the parameters  $R_{\text{HH}}$  and  $\beta$ , which, in the original formulation, respectively represent the distance between two nearest neighbor protons and the width of the Gaussian line due to the dipolar interactions between nonnearest neighbor protons. In a complex system like silk, where no isolated couples of protons are present,  $R_{\text{HH}}$  must be thought as an average parameter.

In the fittings performed by varying all of the parameters, a strong correlation between  $R_{\text{HH}}$  and  $\beta$  was present, preventing precise best-fitting values for both of them from being obtained. FID analyses were therefore performed by fixing  $R_{\text{HH}}$  to the value of 1.83 Å, which was found to give good fittings for all of the FIDs and which is physically meaningful for the systems investigated.

The results obtained for the six samples (naturally hydrated and dry cocoons of the three strains) at 25 °C are reported in Table 1. The decay parameters obtained for the three functions indicate that  $E1$  and  $P$  correspond to very rigid phases, which

do not experience molecular motions with characteristic frequencies higher than kHz, with the possible exception of fast methyl reorientation that, anyway, might only slightly affect proton spin–spin relaxation times.<sup>26</sup> On the contrary, E2, whose  $T_2$  is of the order of 100  $\mu$ s, is representative of a relatively mobile fraction of the samples. Actually, the E2 component is mostly associated to water protons, since it almost vanishes on passing from naturally hydrated to dry samples. Indeed, in dry samples, only about 1% of protons belong to this FID component for Chinese and Turkish cocoons. A separate consideration must be made for the Japanese dry cocoons: in this case, the weight percentage of E2 is much higher (6.6%), and the corresponding  $T_2$  is more than halved with respect to the values obtained for the Chinese and Turkish cocoons. To verify if this diverging result could be ascribable to a strong correlation between the fitting parameters, we repeated the fitting of the relevant FID fixing  $T_{2,E2}$  to the value of 130  $\mu$ s, similar to those obtained for the other samples: this brought to a remarkable increase (about 15%) of the fitting  $\chi^2$ , thus indicating a peculiar behavior for Japanese dry cocoons.

In all of the naturally hydrated samples, the quite short  $T_2$  values for the E2 component (less than 150  $\mu$ s) indicate that water molecules are physisorbed on silk, undergoing restricted reorientational motions, and that no “liquidlike” water is present (for which  $T_2$  values of the order of 1 s would be expected), in agreement with what commonly encountered in biomacromolecular systems.<sup>27,28</sup> The  $w_{E2}$  values for naturally hydrated samples give a quantitative estimate of the percentage of water protons present in these cocoons. In Chinese and Japanese cocoons, this value is about 10.5%, whereas it is about a half for Turkish cocoons: this is consistent with the different behavior observed for the three strains in  $^{13}\text{C}$  CP-MAS spectra, discussed in the previous section, suggesting that the higher amount of water present in naturally hydrated Japanese and Chinese cocoons slightly modifies the CP dynamics of the  $^{13}\text{C}$  Gly peak.

It must be noticed that our FID analysis results are in sensible agreement with those previously reported for silk fibroin<sup>10</sup> and drawn silk<sup>29</sup> samples. In both cases, similar water contents and decay rates were found, even though the most rigid fraction of the sample was described by a single Gaussian function, in place of  $P$  and E1, which, in our case, give a much better reproduction of the FIDs. In particular, a Gaussian function is unable to reproduce the small dip occurring in the experimental FID at about 30  $\mu$ s, which is typical of a Pake function. Indeed, at this stage, it is very difficult to attempt an individual assignment of  $P$  and E1 components, since they both correspond to very rigid phases. However, the nature of the Pake function that should describe more ordered regions, as well as the absence of an exponential component in the FID analyses previously performed on the sole fibroin, strongly suggest that  $P$  and E1 can be roughly assigned to fibroin and sericin, respectively, as also supported by the excellent agreement between the weight percentages of  $P$  and E1 and the relative amounts of fibroin and sericin found for the samples investigated. It is possible to state that, on passing from dry to naturally hydrated samples, the rigid fractions of all of the samples experience a slight but clearly detectable increase of mobility, as indicated by the increase of  $T_{2,E1}$  values (by about 50%, from 17–22 to 26–29  $\mu$ s) and the reduction of  $\beta$  ones (by about 7%, from 51 300–52 600 to 47 300–48 400  $\text{s}^{-1}$ ). This indicates that probably water is mainly adsorbed on hydrophilic sericin, but also, to a minor extent, on amorphous fibroin.

The FID analysis of the three dry samples has been also carried out at different temperatures in the range 25–95  $^{\circ}\text{C}$ , to

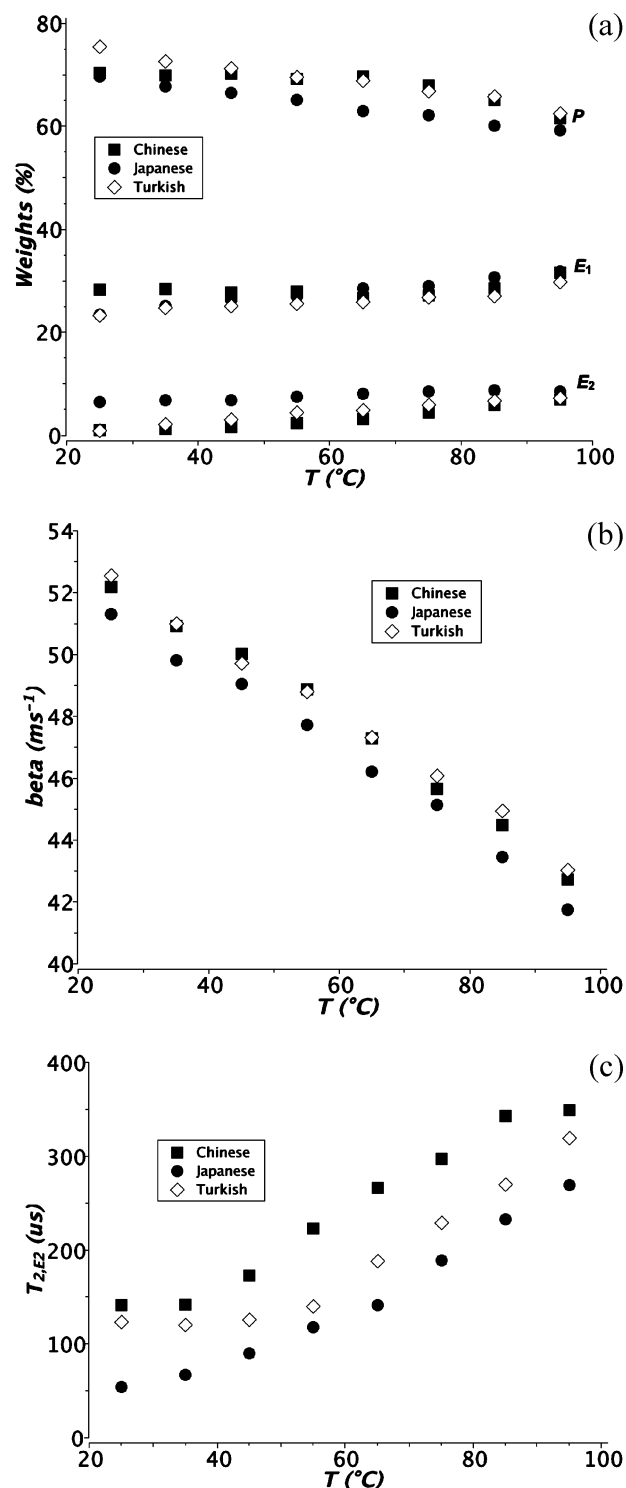


**Figure 4.** Results of the  $^1\text{H}$  FID analyses performed on the dry cocoons at different temperatures. (a) Best-fit weight percentages of the Pake ( $P$ ) and exponential ( $E_1$ ,  $E_2$ ) functions vs.  $T$ . (b) Best-fit  $\beta$  parameter of the Pake function vs.  $T$ . (c) Best-fit  $T_2$  relaxation times for the exponential component  $E_2$  vs.  $T$ .

get a more detailed characterization of the dynamic processes occurring in silk. The results are summarized in Figure 4. It is possible to notice that the trends of the different fitting parameters are very similar for the three samples, with the only exception of the Japanese sample, discussed above. For all of the samples, the weight of the Pake component regularly decreases by increasing temperature, whereas the opposite trend is observed for the  $E_2$  function (which, in dry samples, is ascribable to the most mobile fractions of the proteins),

**Table 2.**  $^1\text{H}$   $T_{1\rho}$  Measurements at 25 °C for Naturally Hydrated (nh) and Dry Cocoons<sup>a</sup>

samples	$w_I$ (%)	$T_{1\rho,I}$ ( $\mu\text{s}$ )	$w_{II}$ (%)	$T_{1\rho,II}$ (ms)	$w_{III}$ (%)	$T_{1\rho,III}$ (ms)	PWRA ( $\text{s}^{-1}$ )
Chinese nh	14.0	601	68.8	6.71	17.2	22.0	343
Japanese nh	14.6	566	70.4	7.60	15.0	23.1	357
Turkish nh	13.6	552	71.1	7.41	15.3	22.0	349
Chinese dry	2.7	325	28.2	5.56	69.1	13.5	185
Japanese dry	8.0	904	92.0	10.2			179
Turkish dry	3.7	283	64.1	7.82	32.2	18.9	230

<sup>a</sup> Maximum estimated error on PWRA is 15%.

indicating that increasing fractions of the sample experience fast motions by furnishing thermal energy. The values of  $\beta$  (see Figure 4b) regularly decrease for all the samples passing from about  $52\,000\text{ s}^{-1}$  at 25 °C to about  $42\,000\text{ s}^{-1}$  at 95 °C and indicating a remarkable increase of mobility within this rigid fraction of the sample. Also the mobility of the most mobile fraction of the sample remarkably increases with temperature, with the value of  $T_{2,E2}$  increasing by a factor of 3–4 from 25 to 95 °C (see Figure 4c). On the contrary, the amount and the mobility of the rigid fraction described by E1 do not seem sensibly affected by temperature, since both its weight ( $\approx 24$ –30%) and  $T_2$  ( $\approx 18$ –22  $\mu\text{s}$ ) values remain substantially constant in the range 25–95 °C.

**$^1\text{H}$   $T_{1\rho}$  Relaxation Times.** To get further insights into molecular dynamic processes occurring in the kHz regime, we performed  $^1\text{H}$   $T_{1\rho}$  measurements on all cocoons at 25 °C. For naturally hydrated cocoons, the  $T_{1\rho}$  decay was well reproduced by a sum of three exponential functions, whereas a good fitting was obtained with two or three exponential functions in the case of dry cocoons, depending on the strain. These findings might appear in disagreement with  $T_{1\rho}$  measurements previously performed on spider silks,<sup>30,11</sup> where a single exponential decay was observed. However, it must be noticed that, in the cases previously reported, the measurements were carried out via  $^1\text{H}$ – $^{13}\text{C}$  CP, rather than through direct low-resolution  $^1\text{H}$  measurements, as in our case. If, on one hand, the method applied by us presents the disadvantage of giving a common response from all the protons in the sample, since no spectral resolution can be exploited, then on the other hand it does not suffer from limitations in the detection of short relaxation components (less than about 1 ms) that in the CP method are prevented by the presence of a nonnegligible contact time. This deviation from a monoexponential decay suggests that heterogeneous domains are present in our samples with average linear dimensions greater than 10–20 Å, as can be estimated from the application of suitable diffusional equations.<sup>31</sup> On the other hand,  $T_{1\rho}$  is very sensitive to dynamic heterogeneities in polymeric systems, and multiexponential  $T_{1\rho}$  decays commonly occur, even in nominally “monophasic” polymers.<sup>32</sup> The  $T_{1\rho}$  measurements performed at 25 °C for all of the samples are reported in Table 2. The three naturally hydrated cocoons show a common behavior, each of the three exponential components exhibiting very similar weights and  $T_{1\rho}$  values. In particular, the presence of a predominant “intermediate” component must be noticed ( $\approx 7$ –8 ms, with a weight of about 70%), which corresponds to the sole component detected in the previous studies, whereas the faster ( $T_{1\rho} \approx 550$ –600  $\mu\text{s}$ ) and slower ( $T_{1\rho} \approx 22$ –23 ms) relaxing components have weights of about 15% each. Chinese and Turkish dry cocoons also experience a triexponential decay, but the weight of the shortest component is in this case reduced to 3–4%. For the Japanese dry cocoons, a biexponential decay is observed, indicating, also in this case, a different behavior with respect to the Chinese and Turkish cocoons. However, the comparison

among the results obtained for the different samples is not straightforward because of the multiexponential behavior, partially affected by proton spin diffusion, the different number of exponential components, and the presence of a different assembly of proton nuclei in the cases of naturally hydrated and dry cocoons. To overcome this difficulty and try to draw some considerations, we made recourse to the population weighted rate average (PWRA),<sup>32</sup> defined as

$$\text{PWRA} = \frac{\sum_i \frac{w_i}{T_{1\rho,i}}}{\sum_i w_i} \quad (6)$$

Indeed, this quantity represents the total power available for relaxation in the rotating frame, it is independent from spin diffusion and, therefore, can be directly related to the dynamic behavior of the system. The values so calculated are reported in Table 2. The PWRA seems to be scarcely affected by the strain, being very similar for the three naturally hydrated samples ( $340$ – $360\text{ s}^{-1}$ ), as well as for the three dry ones ( $180$ – $230\text{ s}^{-1}$ ). The remarkable decrease in PWRA observed on passing from naturally hydrated to dry cocoons could be in principle ascribed to a change in the kHz dynamics or to the loss of the contribution to the relaxation due to water protons. An attempt of further clarifying this point will be performed in the following section, analyzing the results of the  $^1\text{H}$   $T_{1\rho}$ –FID correlation experiments; at this stage, it is possible to state that the combined reduction of PWRA and weight of the shortest  $T_{1\rho}$  component on passing from naturally hydrated to dry samples suggests that the motions occurring in physisorbed water represent an important sink for the spin–lattice relaxation in the rotating frame of the whole spin system.

**$^1\text{H}$   $T_{1\rho}$ –FID Correlation Experiment.** To get additional information on the assignment of FID components and the interpretation of  $^1\text{H}$   $T_{1\rho}$  measurements, we applied the  $^1\text{H}$   $T_{1\rho}$ –FID correlation technique<sup>18</sup> that was already revealed to be particularly useful for either synthetic polymers<sup>33</sup> or biomacromolecules.<sup>27</sup> This experiment was applied to the whole set of naturally hydrated and dry samples at 25 °C. The experiment consists of recording a series of FIDs after application of different spin-lock times (usually at least 30), thus building a two-dimensional data set depending on the acquisition time of the FID on one dimension and on the spin-lock time on the other one. Each of the FIDs so recorded is then reproduced by using the same set of functions previously found from the standard FID analysis by means of a least-squares fit where only the weights of each function are optimized. For each FID function, the weights so obtained are reported as a function of the spin-lock time and fitted to the sum of exponentials previously found from the standard  $^1\text{H}$   $T_{1\rho}$  measurement, obtaining the weights for each  $T_{1\rho}$  exponential as best-fitting parameters. These parameters, one for each  $i,j$  couple, corresponding to the  $i$ th FID and  $j$ th  $T_{1\rho}$  components, are then analyzed following a suitable procedure to obtain three matrices ( $a$ ,  $b$ , and  $c$ ).  $a$  represents the percentage of proton nuclei corresponding to the given FID and  $T_{1\rho}$  components;  $b$ , ranging from  $-1$  to  $+1$ , gives the correlation between the two components ( $-1$ ,  $0$ , and  $+1$  respectively indicate no, average, and complete correlation);  $c$  allows the spin–lattice in the rotating frame relaxation sinks to be identified, being a measure of the weighted relaxation rate corresponding to the selected couple of components.

**Table 3.** Values of the  $b$  Coefficients Indicating the Degree of Correlation between  $^1\text{H}$   $T_{1\rho}$  and FID Components (See Tables 1 and 2), Measured at 25 °C for Naturally Hydrated (nh) and Dry Cocoons

samples	$P-T_{1\rho,I}$	$P-T_{1\rho,II}$	$P-T_{1\rho,III}$	$E1-T_{1\rho,I}$	$E1-T_{1\rho,II}$	$E1-T_{1\rho,III}$	$E2-T_{1\rho,I}$	$E2-T_{1\rho,II}$	$E2-T_{1\rho,III}$
Chinese nh	-1.0	+0.55	+0.24	+0.21	-0.35	+0.07	+0.86	-0.82	-1.0
Japanese nh	-1.0	+0.52	+0.14	+0.05	-0.17	+0.11	+0.86	-0.83	-1.0
Turkish nh	-1.0	+0.49	+0.38	+0.22	-0.28	+0.01	+0.82	-0.77	-1.0
Chinese dry	-1.0	+0.89	+0.01	+0.94	-0.96	+0.01	+0.17	+0.10	-0.33
Japanese dry	-1.0	+1.0		+0.60	-0.58		+0.50	-0.50	
Turkish dry	-1.0	+0.40	-0.07	+0.97	-0.40	+0.05	+0.08	-0.45	+0.30

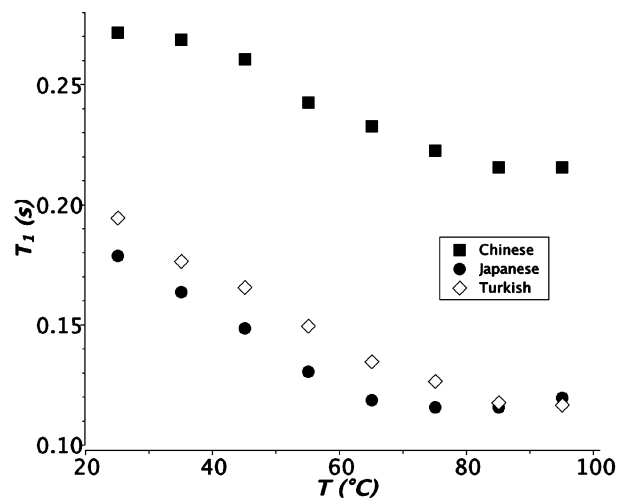
The results obtained for all of the samples at 25 °C are summarized in Table 3, where the  $b$  coefficients are reported for all of the  $T_{1\rho}$ -FID components couples. First of all, it must be noticed that all of the naturally hydrated cocoons give very similar results, highlighting very strong correlations for the couples of components  $P-T_{1\rho,II}$  and  $E2-T_{1\rho,I}$ , and less strong but positive correlations for  $P-T_{1\rho,III}$ ,  $E1-T_{1\rho,I}$ , and  $E1-T_{1\rho,III}$ . It is quite clear that the shortest  $T_{1\rho}$  component ( $T_{1\rho,I}$ ) is mainly associated to water protons (E2) and, to a minor extent, to protons of the E1 FID component. This means that in these two fractions of the samples motions with characteristic frequencies close to the spin-lock frequency (92 kHz) occur, which are absent in the  $P$  fraction, indeed associated only with the two longest  $T_{1\rho}$  components. On dry samples, the results are slightly less homogeneous because of the different number of  $T_{1\rho}$  components determined for the Japanese cocoons and because of the much larger errors obtained for the  $b$  coefficients relative to the E2 FID component, characterized by a very small weight percentage. However, it is very clear that the strongest correlations are, in all cases, for the couples  $P-T_{1\rho,II}$  and  $E1-T_{1\rho,I}$ . The latter, in particular, indicates that, after the removal of physisorbed water, the motions better matching the spin-lock frequency are almost exclusively located into the E1 fraction.

From the calculation of  $c$  parameters, we derived the percentage contributions of the different fractions of the sample to  $T_{1\rho}$  PWRA. In the naturally hydrated samples, about a half of PWRA arises from water protons (E2) and 20–30% from each of the  $P$  and E1 FID components. On the contrary, in dry samples, the contribution of E1 increases up to about 70%, the remaining 30% almost exclusively coming from the  $P$  component.

**$^1\text{H}$   $T_1$  Relaxation Times.** The proton spin-lattice relaxation times in the laboratory frame ( $T_1$ ) have been measured for the dry samples in the temperature range 25–95 °C in order to detect possible differences among the cocoons arising from different silkworm strains in motional processes with characteristic frequencies in the MHz regime. For all samples and at all temperatures, the magnetization recovery was well described by a monoexponential trend, indicating that the averaging effect of spin diffusion is complete in the  $T_1$  time scale. This means that the heterodomains average linear size is of the order of hundreds of Å or less, as it can be derived from the application of suitable diffusional equations.<sup>31,27</sup>

The measured  $T_1$  values for the dry cocoons of the three strains are reported in Figure 5.

All of the relaxation times show a regular decreasing trend by increasing temperature, approaching a minimum at temperatures above 60 °C. This clearly indicates that the molecular motions responsible for spin-lattice relaxation are in a slow motional regime (that is the characteristic frequencies of the motions are lower than the Larmor frequency of 25 MHz) at room temperature but tend to reach an intermediate regime (characteristic frequencies of the order of 25 MHz) at the highest temperatures investigated. However, both the temperature at

**Figure 5.**  $^1\text{H}$  spin-lattice relaxation times in the laboratory frame ( $T_1$ ) measured on the dry cocoons at different temperatures. Maximum estimated experimental error on  $T_1$  values is 2%.

which the  $T_1$  minimum occurs (about 75, 85, and above 95 °C for Japanese, Chinese, and Turkish cocoons, respectively) and the  $T_1$  values at each temperature strongly differ from strain to strain, indicating that a different molecular dynamics in the MHz regime is experienced. To verify if these differences could be really ascribed to the different strain, we repeated some of the measurements for different individuals of the same strain:  $T_1$  values differing at most by 7% from their average value were determined, indicating a strong individual dependence, that is, however, less than the differences observed between cocoons belonging to different strains.

The identification of the motional process mainly responsible for proton  $T_1$  relaxation at 25 MHz in the temperature range investigated is not straightforward. Previous studies performed on polypeptides<sup>34</sup> and silk fibroin<sup>10</sup> have highlighted the predominant contribution, below 250 K, of alanine methyl fast reorientations. At higher temperatures, these motions become too fast to effectively contribute to spin-lattice relaxation, and the main contribution arises from reorientational motions of water molecules. However, it was shown that in dry fibroin the most important contribution to relaxation times measured at a Larmor frequency of 90 MHz remains that of methyl reorientations, and therefore, the relaxation times keep increasing by increasing the temperature up to about 120 °C, where they approach a maximum at  $T_1$  values of about 1–2 s, indicating that another motional process is mainly responsible for relaxation at higher temperatures.<sup>10</sup> In our case, the measurements are performed at a much lower Larmor frequency (25 MHz), and therefore, the relaxation curve arising from the methyl reorientations and, consequently, the  $T_1$  maximum, is shifted toward lower temperatures.<sup>35</sup> What we observe in the temperature range investigated is mainly the effect of a motional process slower than methyl reorientations, which in higher-frequency measurements is most effective only above 120 °C. On the basis of the

$^{13}\text{C}$  DE-MAS spectra recorded with a short relaxation delay (Figure 2), we can tentatively identify it with the reorientation of serine  $\text{CH}_2\text{OH}$  groups that in our systems should remarkably contribute to proton relaxation because of the presence of serine-rich sericin. However, the certain identification of this process, as well as its quantitative characterization, will require additional efforts, both performing measurements on "model" or suitably treated samples, and analyzing a much wider set of experimental data, collected for different nuclei and at different Larmor frequencies, as recently revealed necessary for polymeric systems.<sup>32,35–37</sup> This is beyond the scope of the present study, and it will be the subject of a future work. However, it is clear that proton  $T_1$  is the most sensitive nuclear parameter, being somewhat both individual and strain-dependent. Since the differences here observed in the  $T_1$  trends of cocoons arising from different strains are larger than those arising from different individuals of the same strain, these measurements seem promising for highlighting strain-dependent cocoon properties at a molecular level.

### Conclusions

In this paper, a combination of solid-state NMR techniques has been applied to characterize and compare the dynamic behavior at a molecular level of silkworm cocoons produced by three different *Bombyx mori* strains. Different low-resolution ( $^1\text{H}$  FID analysis,  $^1\text{H}$  spin-lattice relaxation time measurements in both rotating and laboratory frames,  $^1\text{H}$  FID- $T_{1\rho}$  correlation experiment) and high-resolution ( $^{13}\text{C}$  spectra recorded by CP- and DE-MAS experiments) techniques were applied on both naturally hydrated and dry samples, in some cases at different temperatures, to get information on motional processes occurring at different characteristic frequencies, as well as to investigate the effect of both temperature and hydration on such processes.

In general, three domains with different dynamic behavior can be detected, corresponding to the three functions (one Pake and two exponentials), whose linear combination reproduces the proton free induction decay. They roughly correspond to rigid fibroin and sericin and to a mobile fraction, which becomes important only above room temperature or in the presence of physisorbed water. A higher mobility is induced either in fibroin domains by increasing temperature or in both fibroin and sericin fractions by water, which indeed seems to be physisorbed on both sericin and amorphous fibroin.

Motions in the MHz range only involve side-chain moieties, and, in particular, alanine  $-\text{CH}_3$  and serine  $-\text{CH}_2\text{OH}$  groups. The most important motions in the kHz regime are, instead, those occurring in physisorbed water (contributing for about a half of the total relaxation power in naturally hydrated cocoons) and, to a minor extent, in sericin.

The cocoons arising from different strains generally show a similar behavior, but some detectable differences concern the different amount of physisorbed water (lower for the cocoons of the Turkish strain), the dynamic properties in the kHz regime (peculiar for the dry cocoons of the Japanese strain), and those in the MHz regime, which reveal to be very sensitive to the different strains but also, even though to a minor extent, to different individuals of the same strain.

Finally, despite the fact that several of the results obtained here need a deeper investigation and interpretation, it is possible to state that the combined application and analysis of the different solid-state NMR techniques here reported appear very promising in elucidating the molecular motional processes occurring in very complex biomacromolecular systems, such as silkworm cocoons, in the perspective of understanding the molecular mechanisms determining their macroscopic properties.

**Acknowledgment.** The authors thank Prof. C. A. Veracini, Dr. L. Cappellozza, Dr. M. Masetti, and Dr. S. Faragò for useful discussions.

### References and Notes

- (1) Zhao, C.; Asakura, T. *Prog. Nucl. Magn. Reson. Spectrosc.* **2001**, *39*, 301–352 and references therein.
- (2) Yao, J.; Nakazawa, Y.; Asakura, T. *Biomacromolecules* **2004**, *5*, 680–688.
- (3) Asakura, T.; Suita, K.; Kameda, T.; Afonin, S.; Ulrich, A. S. *Magn. Reson. Chem.* **2004**, *42*, 258–266.
- (4) Ashida, J.; Ohgo, K.; Asakura, T. *J. Phys. Chem. B* **2002**, *106*, 9434–9439.
- (5) Nakazawa, Y.; Asakura, T. *J. Am. Chem. Soc.* **2003**, *125*, 7230–7237.
- (6) Kishi, S.; Santos, A., Jr.; Ishii, O.; Ishikawa, K.; Kunieda, S.; Kimura, H.; Shoji, A. *J. Mol. Struct.* **2003**, *649*, 155–167.
- (7) Gullion, T.; Kishore, R.; Asakura, T. *J. Am. Chem. Soc.* **2003**, *125*, 7510–7511.
- (8) Asakura, T.; Sugino, R.; Yao, J.; Takashima, H.; Kishore, R. *Biochemistry* **2002**, *41*, 4415–4424.
- (9) Ashida, J.; Ohgo, K.; Komatsu, K.; Kubota, A.; Asakura, T. *J. Biomol. NMR* **2003**, *25*, 91–103.
- (10) Asakura, T.; Demura, M.; Watanabe, Y.; Sato, K. *J. Polym. Sci.: Part B Polym. Phys.* **1992**, *30*, 693–698.
- (11) Kishore, A. I.; Herberstein, M. E.; Craig, C. L.; Separovic, F. *Biopolymers* **2002**, *61*, 287–297.
- (12) Kongdee, A.; Bechtold, T.; Teufel, L. *J. Appl. Polym. Sci.* **2005**, *96*, 1421–1428.
- (13) Krushelnitsky, A.; Reichert, D. *Prog. Nucl. Magn. Reson. Spectrosc.* **2005**, *47*, 1–25.
- (14) Zhang, Y.-Q. *Biotechnol. Adv.* **2002**, *20*, 91–100.
- (15) Cho, K. Y.; Moon, J. Y.; Lee, Y. W.; Lee, K. G.; Yeo, J. H.; Kweon, H. Y.; Kim, K. H.; Cho, C. S. *Int. J. Biol. Macromol.* **2003**, *32*, 36–42.
- (16) Doira, H. Genetic stocks of the silkworms. In *The silkworm: an important laboratory tool*; Tazima, Y., Ed.; Kodansha: Tokyo, 1978; pp 53–81.
- (17) Cory, D. G.; Ritchey, W. M. *J. Magn. Reson.* **1988**, *80*, 128–132.
- (18) Geppi, M.; Kenwright, A. M.; Say, B. J. *Solid State NMR* **2000**, *15*, 195–199.
- (19) Asakura, T.; Yao, J. *Protein Sci.* **2002**, *11*, 2706–2713.
- (20) Holland, G. P.; Lewis, R. V.; Yarger, J. L. *J. Am. Chem. Soc.* **2004**, *126*, 5867–5872.
- (21) Yang, Z.; Liivak, O.; Seidel, A.; LaVerde, G.; Zax, D. B.; Jelinski, L. W. *J. Am. Chem. Soc.* **2000**, *122*, 9019–9025.
- (22) Hansen, E. W.; Kristiansen, P. E.; Pedersen, N. J. *Phys. Chem. B* **1998**, *102*, 5444–5450.
- (23) Pake, G. E. *J. Chem. Phys.* **1948**, *16*, 327–336.
- (24) Look, D. C.; Lowe, I. J.; Northby, J. A. *J. Chem. Phys.* **1966**, *44*, 3441–3452.
- (25) Abramowitz, M.; Stegun, I. *Handbook of Mathematical Functions*; Dover: New York, 1970.
- (26) McBrierty, V. J.; Douglass, D. C.; Falcone, D. R. *J. Chem. Soc., Faraday Trans. 2* **1972**, *68*, 1051–1059.
- (27) Calucci, L.; Galleschi, L.; Geppi, M.; Mollica, G. *Biomacromolecules* **2004**, *5*, 1536–1544.
- (28) Calucci, L.; Forte, C.; Galleschi, L.; Geppi, M.; Ghiringhelli, S. *Int. J. Biol. Macromol.* **2003**, *32*, 179–189.
- (29) Tanaka, T.; Kobayashi, M.; Inoue, S.-I.; Tsuda, H.; Magoshi, J. *J. Polym. Sci.: Part B Polym. Phys.* **2003**, *41*, 274–280.
- (30) Simmons, A.; Ray, E.; Jelinski, L. W. *Macromolecules* **1994**, *27*, 5235–5237.
- (31) McBrierty, V. J.; Packer, K. J. *Nuclear Magnetic Resonance in Solid Polymers*; Cambridge University Press: Cambridge, U.K., 1993.
- (32) Geppi, M.; Harris, R. K.; Kenwright, A. M.; Say, B. J. *Solid State NMR* **1998**, *12*, 15–20.
- (33) Ferrini, V.; Forte, C.; Geppi, M.; Pizzanelli, S.; Veracini, C. A. *Solid State NMR* **2005**, *27*, 215–222.
- (34) Andrew, E. R. *Polymer* **1985**, *26*, 190–192.
- (35) Forte, C.; Geppi, M.; Malvaldi, M.; Mattoli, V. *J. Phys. Chem. B* **2004**, *108*, 10832–10837.
- (36) Moe, N.; Qiu, X. H.; Ediger, M. D. *Macromolecules* **2000**, *33*, 2145–2152.
- (37) Qiu, X. H.; Moe, N. E.; Ediger, M. D.; Fetters, L. J. *J. Chem. Phys.* **2000**, *113*, 2918–2926.